

# Ion Thruster Optical Performance Enhancement via Ion-emissive-surface Shaping

IEPC-2005-95

Presented at the 29<sup>th</sup> International Electric Propulsion Conference, Princeton University,  
October 31 – November 4, 2005

Paul J. Wilbur<sup>\*</sup>, Cody Farnell<sup>†</sup>, and John D. Williams<sup>‡</sup>

Colorado State University  
Fort Collins, Colorado, 80523, USA

**Abstract:** Numerical results that demonstrate how ion emissive surfaces should be shaped to induce the formation of well-focused, high-current beamlets are presented. Results obtained when the sheath shape and position are established and then held constant as operating conditions are changed are compared to corresponding results obtained with a conventional plasma sheath that moves. These comparisons show the shaped surface: 1) yields beamlets that remain focused over wider beamlet current ranges, 2) enables operation without a crossover limit, and 3) enables operation at lower net-to-total accelerating voltage ratios and, therefore, at lower specific impulses. It is also shown that even greater beamlet currents can be extracted before the perveance limit is encountered if the propellant utilization efficiency approaches 100% and it is no longer necessary to have a small accel hole diameter to limit neutral propellant loss. Such a propellant utilization efficiency is expected for the Emissive Membrane Ion Thruster because its membrane is able to pass only ionized propellant.

|          |   |
|----------|---|
| d        | = diameter ( $d_s$ – screen, $d_a$ – accel, $d_d$ - decel)            |
| E        | = electric field strength   |
| J        | = current ( $J_b$ – beamlet, $J_i$ – impingement)                     |
| r        | = radius ( $r_s$ – screen, $r_a$ – accel)                             |
| $\ell_g$ | = grid spacing  |
| u        | = Bezier function independent variable                                |
| V        | = voltage ( $V_a$ – accel, $V_d$ – decel, $V_N$ – net, $V_T$ – total) |
| z        | = axial position  |

## I. Introduction

An attractive feature of conventional, gridded electron bombardment ion thrusters in comparison to other electric propulsion devices is the separability of the various processes (ionization, ion acceleration, and neutralization) that are essential to their operation. This separability enables relatively independent control and optimization of each process that in turn enables efficient thruster operation over a wide range of thrust and specific impulse with a variety of propellants. One aspect of thruster operation that is not controllable, however, is related to the sheath from which ions are accelerated into beamlets. As discharge plasma conditions change in these thrusters, the sheaths change in both shape and position. These shape and position changes are problematic because they lead to beamlet defocusing and give rise to ion trajectories that impinge on and sputter erode the accelerator grid. They thereby limit the range of beamlet currents that can be extracted without degrading thruster lifetime. It is; however, possible to extend this range if the ions are drawn from an emissive surface that is properly shaped and

---

<sup>\*</sup> Professor, Department of Mechanical Engineering, pwilbur@engr.colostate.edu.

<sup>†</sup> Research Asst., Department of Mechanical Engineering, ccf@engr.colostate.edu.

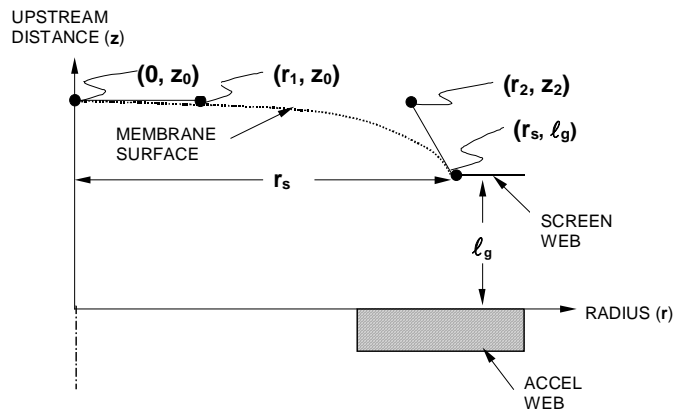
<sup>‡</sup> Asst. Professor, Department of Mechanical Engineering, johnw@engr.colostate.edu.

retains both its shape and position as operating conditions change. Qualitative evidence that emissive surface shape and position control can be used to control ion beamlet focusing is found in at least two ion source applications. Specifically, contact ion thrusters that utilized ion emission from a shaped porous tungsten surface<sup>1</sup> and more recently tungsten wire meshes<sup>2</sup> that constrained changes in conventional discharge plasma sheaths. For the wire mesh case and probably for the contact thruster<sup>3</sup> as well surface shape optimization appears to have been accomplished empirically. A quantitative study of the benefits of an optimally shaped and positioned emissive surface that clearly demonstrates its benefits is, therefore, needed. The understanding obtained from such a study could enhance the performance of contact and constrained-sheath ion optics systems but simulations performed herein are directed mostly at prediction of the ion optical performance that might be obtained from the recently proposed Emissive Membrane Ion Thruster (EMIT)<sup>4</sup>.

## II. Numerical Approach

The basis of the numerical simulations used in this study is the ffx code<sup>5</sup> developed to model the ion optical behavior of beamlets in conventional electron-bombardment ion thrusters. In conducting this study the code was used in its standard form to model conventional plasma sheath optics cases for comparison to defined emissive surface cases. Modifications were made to the code so it could also be used to model ion emission at a uniform current density from a definable, uniform-potential surface. The shape of this surface, which may be envisioned as a thin membrane, was defined using a four-control-point Bezier function<sup>6</sup> to locate the points on the cross section of the surface through its centerline of revolution. The geometry of a typical membrane cross section relative to standard screen and accel grid webbing reference points and the beamlet centerline is shown in Fig. 1. As the figure suggests, positions on the emission surface are located relative to the centerline in the radial ( $r$ ) direction and relative to the upstream plane of the accel grid surface in the axial ( $z$ ) direction. The four-control-point Bezier function is well suited to the task of defining the membrane cross section because it yields a smooth curve through specified end points at specified end-point slopes. In this case the end points are on the centerline at  $(0, z_0)$  and at the outer edge of membrane  $(r_s, \ell_g)$ . It is argued that the surface slope at the centerline should be zero to obtain minimum ion beamlet divergence. The centerline control point  $(0, z_0)$  together with the next one  $(r_1, z_0)$  define this centerline slope and the membrane flatness in this region. The other free control point  $(r_2, z_2)$  defines the slope and rate of slope change near the outer edge of the surface. When values for the four free control coordinates ( $z_0$  in two places,  $r_1, r_2$  and  $z_2$ ) together with the prescribed ones  $(0, r_s,$  and  $\ell_g)$  are put into the equations as shown on Fig. 1 locations of any point on the surface can be calculated. The calculation is performed in terms of the Bezier independent variable ( $u$ ) where  $0 \leq u \leq 1$ . Optimization of the sheath shape to realize a particular operational goal (e.g. maximum beamlet current or minimum divergence) is accomplished by changing the four free control points ( $z_0, r_1, r_2,$  and  $z_2$ ).

The ffx code utilizes random release of ions from an upstream plane to perform ion optics analysis. Hence, with this feature unmodified the arrival and immediate release rate of ions from the uniform potential emissive surface would have been greater near the emissive surface centerline than at its edge. This is a consequence of a surface slope that is lower near the center of the surface than it is at the edge. Uniform emission current density is required, however, to model EMIT concept<sup>4</sup> behavior. Hence the upstream plane release approach was retained for simulation of conventional beamlets that utilize ions drawn from a plasma and a new section of code that yields uniform emission over the prescribed surface was added to it to simulated the EMIT cases.



Bezier Equations:

$$z = (1 - u)^3 z_0 + 3(1 - u)^2 u z_0 + 3(1 - u) u^2 z_2 + u^3 l_g$$

$$r = (1 - u)^3 0 + 3(1 - u)^2 u r_1 + 3(1 - u) u^2 r_2 + u^3 r_s$$

Fig. 1 Bezier Function Description of Membrane Surface Cross Section

### III. Simulation Space

Experimental work being done on the EMIT concept stimulated interest in the study reported in this paper. Because that work utilized an emissive membrane with a radius ( $r_s$ ) of 3.2 mm, that radius was used for most of the numerical simulations. Other grid parameter values (intragrid electric field [E], accel grid diameter and thickness, etc.) were scaled from this value of  $r_s$  based on current (NSTAR) design values. The same grid dimensions and voltages were used for simulations on both conventional and emissive surface (EMIT) grids so results for these grid sets could be compared. Two regimes of operation defined by specific impulses of interest were investigated. One was at the highest value consistent with prevention of electron backstreaming and the scaled grid system parameters defined by E and  $r_s$  (7500 sec). For these simulations a two-grid system was modeled and accel grid voltages were selected to provide about a 45-V margin against electron backstreaming.

The other specific impulse selected for study was a low one (1500 sec). It was selected so it would be well below the range in which state-of-the-art electron bombardment ion thrusters can operate efficiently. In these cases a low net acceleration voltage ( $\sim 150$  V) was required and a large screen hole radius was neither necessary nor desirable. A common screen grid radius ( $r_s$ ) of one millimeter was selected as a reasonable value for fabrication of a conventional grid set even though smaller holes are readily fabricated in the EMIT configuration. The intragrid electric field was, however, maintained at the same value used for the high specific impulse study to enable high current density operation. At this condition the accel grid was biased to very large negative voltages where the net-to-total accelerating voltage ratios are small (0.11 for this design). Under these conditions electron backstreaming does not occur, but extracted beamlets tend to be very divergent. Preliminary simulations were run with two-grid systems for the conventional and EMIT configurations. In both cases the divergence angles based on 95% current enclosure approached  $90^\circ$ . As a result it was concluded that three-grid systems, which are known to improve focusing in such cases<sup>7</sup>, should be used for the comparison study. The third (grounded) decel grid that was added had the same thickness and hole diameter as the conventional screen grid and the separation between the accel and decel grids was the same as that between the screen and accel grids.

The charge-to-mass ratio of singly charged xenon was used in all of the simulations so results could be compared readily to the large body of work that has been done with this propellant and on the basis that EMIT would ultimately use a propellant with a similar charge-to-mass ratio. For all simulations of conventional ion thruster optics a propellant utilization efficiency of 87% was used because it is considered typical. For the emissive surface cases theory and experiment both suggest the utilization efficiency will be substantially greater than this and may be essentially 100%. For the purposes of this study a value of 98% was selected for the EMIT case on the assumption that some unrecognized mechanism of charge exchange effects might evolve.

### IV. Results

The values of the free Bezier control points used for the EMIT grids were selected by varying them one at a time in 0.1 mm increments to find those values that gave the emissive surface shape that yielded maximum perveance-limited beamlet current. The control points were then varied a final time with these same increments to assure that the free control point final values yielded at least a local optimum. Once the optimum Bezier control points had been determined these values were held fixed and EMIT grid optical performance was examined over its full range to the perveance limit. For the conventional grid, the sheath shape and position adjust automatically and performance analysis in these cases simply involved simulation at beamlet currents over the range between the crossover and perveance limits.

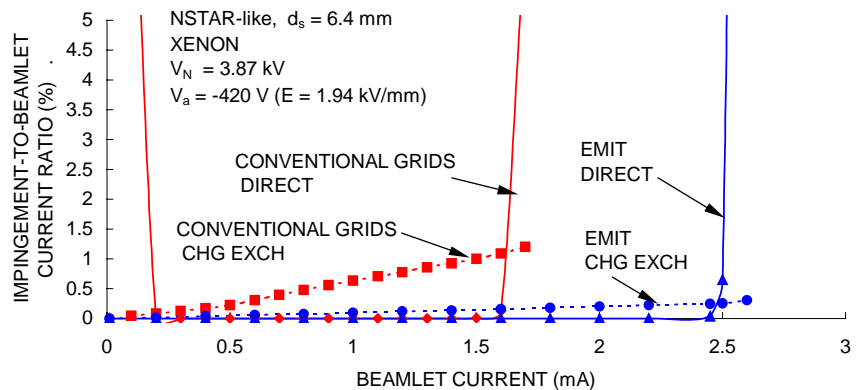


Fig. 2 Beamlet Performance Comparison for Conventional and Emissive Membrane Grids at a High Specific Impulse Operating Condition

### A. High Specific Impulse Operation

Plots of impingement-to-beamlet current ratio v. beamlet current computed at the high specific impulse operating condition are shown in Fig. 2. The direct and charge exchange impingement currents have been plotted separately to show the beneficial effect of the greater propellant utilization efficiency of the EMIT configuration and so the consequence of 100% utilization could be seen by disregarding the EMIT charge-exchange line. Comparison of the data for the two grid sets shows EMIT charge exchange impingement currents that are 1/6 to 1/7 those of the conventional grids. The solid red line shows the conventional grids exhibit crossover and perveance limits (sharp rises in impingement-to-beamlet current ratio) near 0.2 and 1.6 mA, respectively. The EMIT grids, on the other hand, show much better performance in which no crossover behavior occurs and the perveance limit is near 2.5 mA. The reasons for the more than 50% increase in perveance limit and elimination of crossover behavior with EMIT can be understood by considering the shapes and positions of the emissive surface (EMIT) and the conventional grid

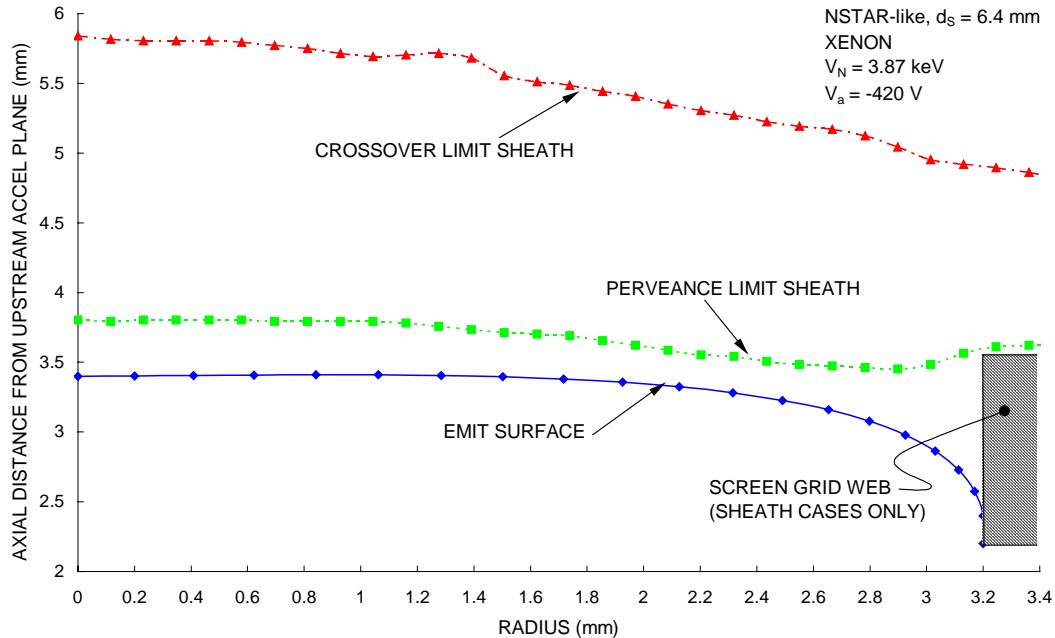


Fig. 3 Sheath and Emissive Surface Comparison at a High Specific Impulse Operating Condition

sheaths shown in Fig.3. They suggest:

1) Crossover occurs when extraction from plasma is involved because the sheath moves upstream and flattens to the point where it no longer focuses the ions properly. The EMIT surface does not change shape or move as beamlet current changes; as a result the ion trajectories do not change substantially and the beamlet stays focused.

2) A major reason why the EMIT optics realizes a greater perveance limit is probably because it is closer to the accel grid than the perveance limit plasma sheath. In other words, EMIT optics enable the benefit of a zero thickness screen grid without its structural and focusing disadvantages.

It is also noteworthy that the optimum EMIT surface shape for maximum perveance operation has almost infinite slope at the edge of the region of beamlet extraction and therefore releases ions on essentially radially **inward** trajectories. It is interesting to contrast this behavior with the complicating effect of the Debye-length-related sheath displacement from the edge of the screen grid. This displacement causes the ions at the edge of the sheath to have radially **outward** velocity components and probably results in direct ion impingement on and lifetime degradation of the accel grid.

Additional qualitative physical understanding of the differences between the focusing and neutralization behaviors of the two grid sets can be seen in Fig. 4. It shows the emissive surface and the sheath shapes (red meshes), the shapes of neutralization surfaces (blue meshes), and beamlet ion density maps referenced to an accel grid. The EMIT surface (red mesh) is common to all EMIT currents and is shown only at the top of the EMIT column. The accel grid beneath it represents a common reference for the neutralization and beamlet density maps

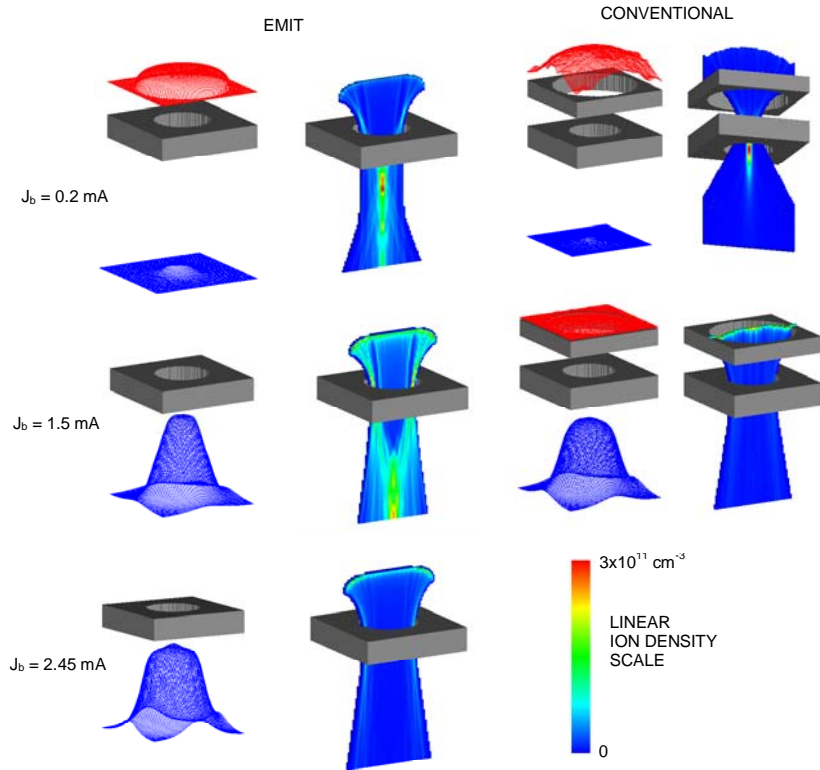


Fig. 4 Beamlet, Sheath and Emissive Surface Comparisons for High Specific Impulse Operation

shown throughout the rest of the figure. Each sheath for a conventional grid set is shown with its neutralization surface just beneath it and to the left of its corresponding beamlet.

Each red and blue mesh pair is to the left of its corresponding beamlet so it can be seen without the interference of the beamlet. The beamlets are actually ion density maps on a plane that includes the beamlet centerline. The beamlet currents given on the far left are (in top-to-bottom order) the conventional grid crossover and perveance limit values as well as the perveance limit value for the EMIT grid. In addition to showing the same

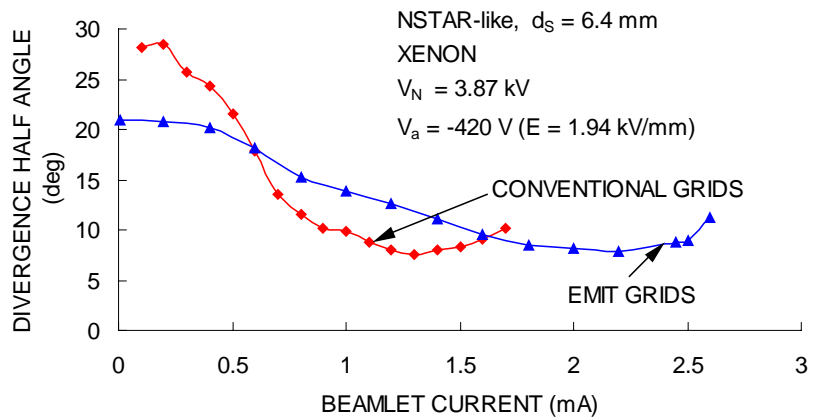


Fig. 5 Comparison of Divergence Half Angles (95% enclosure criterion)

sheath shapes and positions as Fig. 3, these results show the EMIT beamlets remain very similar in shape as the beamlet current changes. On the other hand, the shape of the conventional grid beamlets changes significantly over its range of operation. The differences in the neutralization surfaces are seen to be relatively modest.

Figure 5 shows the effect of changes in beamlet current on the divergence half angle (based on enclosure of 95% of the beam ions) for the two grid sets. As expected the EMIT beamlets exhibit lower divergence than the conventional ones at low beamlet currents because the fixed emission surface sustains a focused beamlet while the conventional sheath surface moves and distorts and hence defocuses its beamlet. Both schemes exhibit similar divergence magnitudes and behaviors near their respective perveance limits. It should be noted here that the EMIT surface shape was optimized for maximum beamlet current and it is anticipated that lower divergence half angles would be realized if it had been optimized for minimum divergence.

### 1. Propellant Utilization Related Effects

The immediately obvious benefits of operation at a high propellant utilization efficiency are the direct propellant mass savings and the increase in thruster lifetime that is a result of the associated reduction in charge exchange ion production. A less obvious advantage of removing the discharge chamber as a source of neutral propellant is elimination of the requirement that the accel grid hole be small enough to limit neutral propellant losses to an acceptably low level. In order to quantify this benefit, simulations that produced results like those shown in Fig. 2 were performed for EMIT grid sets having accel hole diameters ranging from 3.8 mm to 6.4 mm (the screen hole diameter). At each diameter the Bezier control points were varied to optimize the emissive surface shape for the maximum beamlet current. The resulting values of perveance-limited beamlet current, which are shown in Fig. 6a, exhibit a linear variation with accel hole diameter. The maximum value (4.8 mA) is three times that for the conventional grid set operating with the same net accelerating voltages and with all grid dimensions being the same except accel grid hole diameter. The price that must be paid for this increase in beam current is an increase in beamlet divergence half angle and in the accel grid voltage required to prevent electron backstreaming through the larger diameter accel hole. The extents of these increases are shown in Figs. 6b and c. It should be noted that the increase in accel voltage is probably not a significant concern in this case because charge exchange ion production with its attendant erosion should become small, possibly approaching zero, as the propellant utilization efficiency approaches 100%.

As the accel hole diameter is increased Fig. 6a shows greater beamlet currents flow at the perveance limit. In order to pass this additional current with its greater space charge effects, the simulations indicate the optimum emissive surface shape must change. The nature of these changes, which are shown in Fig. 7, is complex and involves both axial movement of the centerline position and the shape of the emissive surface. It is noteworthy that the centerline position of the sheath moves first downstream and then upstream as the hole diameter and perveance-limited beamlet current is increased.

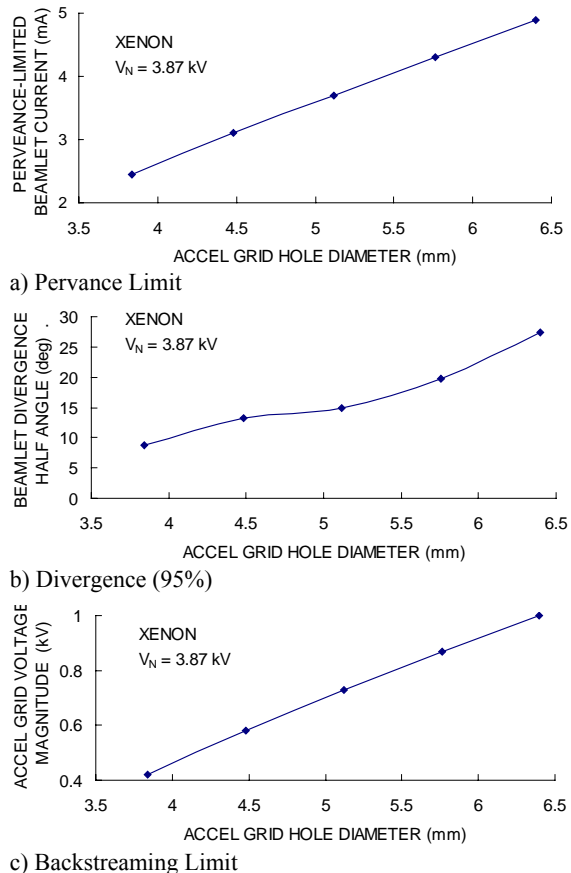


Fig. 6 Effect of Accel Hole Diameter on EMIT Grid System Performance at High Specific Impulse

## B. Low Specific Impulse Operation

The EMIT and conventional electron bombardment thruster three-grid optics systems used for this part of the study were scaled down from the high specific impulse grid set in the ratio of their screen-grid diameters (i.e.  $2/6.4 = 31\%$ ). In addition to the low net accelerating voltage they required for 1500 s specific impulse operation they were operated at a very low net-to-total accelerating voltage. Typical plots of impingement-to-beamlet current ratio  $v.$  beamlet current for these grids, which are shown in Fig. 8, are similar to those obtained for the high specific impulse grids. Specifically, the conventional grids exhibit both crossover and perveance limits (0.02 and 0.24 mA, respectively) and the EMIT grids show no crossover behavior and a perveance limit (0.3 mA) that is 25% greater than that for the conventional grids. Also, the impingement current for the EMIT grids (dotted blue) is substantially lower than that for the conventional grid set (dotted red). The beamlet currents are an order of magnitude lower than they were for the high specific impulse cases because their screen hole area is an order of magnitude lower for these smaller (2-mm diameter) screen grid holes. Note the electric field is the same for both the high and low specific impulse grid sets.

The beamlet divergence behavior of the EMIT and conventional grids are compared in Fig. 9. As with the high specific impulse ones, these grid sets have divergence half angles (based on enclosure of 95% of the beamlet ions) that are of similar magnitude. The EMIT grid is, however, better behaved in that it shows divergence angle amplitude fluctuations that are lower than those of the conventional grid do. Recall that the divergence angles shown are probably not the lowest that could be achieved with the EMIT grids because the surface shape was optimized for maximum beamlet current rather than minimum divergence.

Still, the EMIT grid divergence half angles of Fig. 9 are probably acceptable for many low specific impulse applications. In this regard it is important to recall that the specific impulse for the case studied is very low (1500 sec) and operation becomes more efficient as specific impulse is allowed to increase.

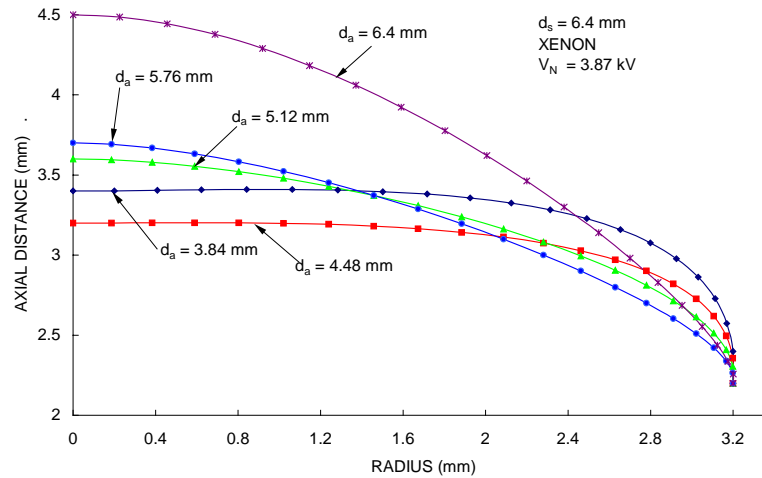


Fig. 7 Effect of Accel Hole Diameter on Optimal Emissive Surface Shape

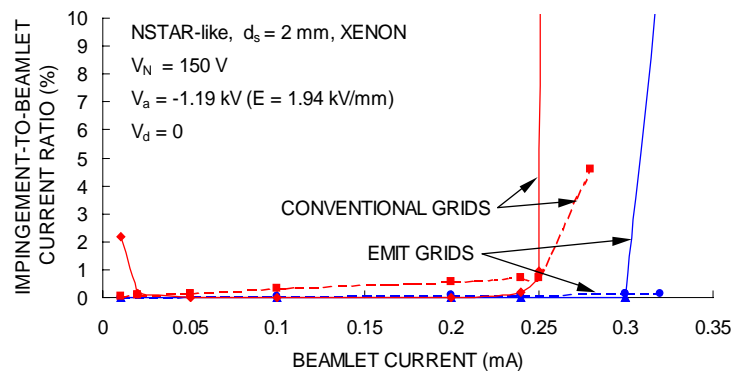


Fig. 8 Perveance and Crossover Limit Comparison at Low Specific Impulse Operating Conditions

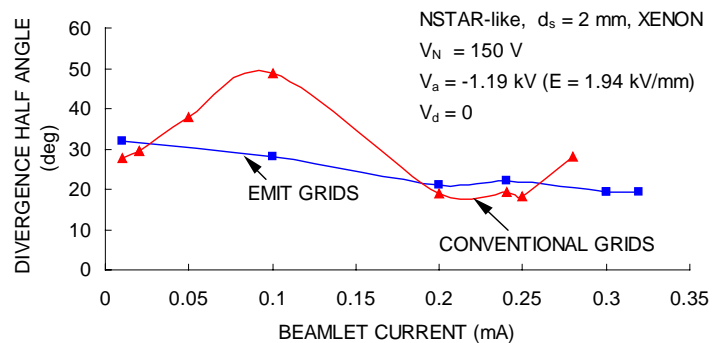


Fig. 9 Divergence Comparison for Low Specific Impulse Operation

The simulation data also show the significant degradation in the electrical efficiency of the thruster with conventional grids that can be expected at the low specific impulse conditions. The reason for this is shown in Fig. 10, which is a plot of the ion current that can be expected to flow to the screen grid rather than passing through it. This screen grid current, which has been normalized using beamlet current, is seen to rise from about 20% of the at the crossover limit to over 100% at the perveance limit. On the other hand there is no such loss with the EMIT grid because its operation does not rely on ion extraction from a plasma through a screen grid hole. Rather, all ions are produced in a membrane and are emitted and accelerated to form the beamlet from the surface of that membrane.

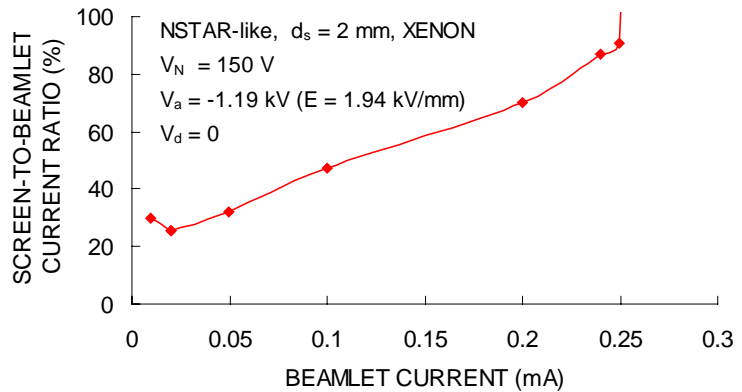


Fig. 10 Ion Current Loss to Screen Grid with Conventional Grids Operating at Low Specific Impulse Condition

No simulations were carried out with increased accel hole diameters for the low-specific impulse operating conditions. It is expected, however, that such increases would enable increases in the perveance limited beamlet current coupled with increases in beamlet divergence half angle that could well be more substantial than they were in the high specific impulse cases. Because the high voltages applied to the accel grid are already very high at the low specific impulse operating conditions investigated here, it is unlikely that they would have to be changed to limit electron backstreaming as accel hole diameter was increased.

Examples of the 3-grid configurations for the EMIT and conventional thruster systems are compared in Fig. 11. The comparisons are shown at beamlet currents of 0.1 mA (conventional grid crossover limit), 0.24 mA (conventional grid perveance limit) and only the EMIT at its perveance limit (0.3 mA). As for Fig. 4, the EMIT surface (red mesh) is common to all EMIT currents and is shown only at the top of the EMIT column. Beneath it are the accel and decel grids, which are common and provide positional reference for each beamlet and sheath. The sheaths for the conventional grids are shown just above each corresponding beamlet picture so they can be studied without the visual interference of superimposed beamlet data. The beamlets are shown as ion density maps on a plane that includes the beamlet centerline. No neutralization surfaces are shown because the very negative accel grid assures they are both far downstream and flat in each case.

The axial movement and shape change of the conventional sheath between the 0.1 and 0.24 mA limits can be seen. The current of ions flowing to the screen grid of the conventional grids is also apparent. In general the EMIT beamlet maps reveal ion densities that are more uniform.

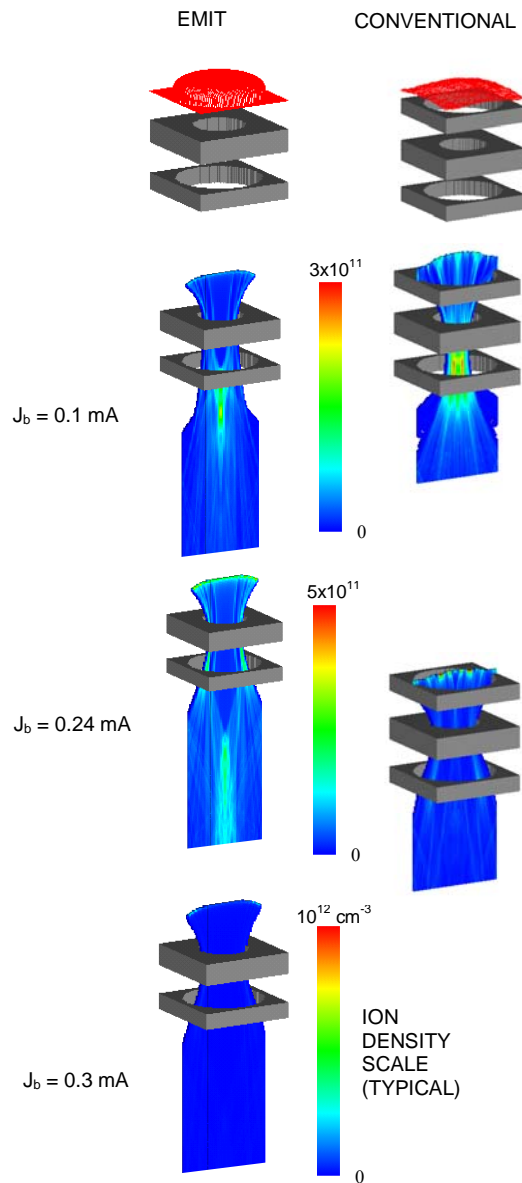


Fig. 11 Low Specific Impulse (3-grid) Beamlet Comparisons

## V. Conclusion

Ions emitted into beamlets from a fixed, designable (EMIT) surface rather than from the plasma sheaths of conventional ion thrusters enable significant improvements in performance. Specifically, the crossover limit on the EMIT beamlet current is eliminated and the current that can be extracted at its perveance limit is increased 25 to 50% above that for a conventional (plasma source) beamlet. The elimination of the crossover limit is a direct result of the fact that a membrane emissive surface remains fixed in both shape and position while a plasma sheath moves and distorts with changes in beamlet current. Since the emissive membrane is expected to transmit only ions (i.e. essentially no neutral atoms) to its downstream surface, additional concerns associated with charge exchange ion production and the associated accel grid erosion are eliminated. In this case the accel hole diameter can be increased and this in turn enables a three-fold increase in the perveance limit. Such changes necessitate corresponding

increases in the magnitude of the accelerator grid voltage and the ion beamlet divergence half angle. Surface emission also facilitates efficient and reasonably well-focused ion beamlet extraction at significantly lower specific impulses than can be achieved using state-of-the-art electron bombardment thrusters. These findings support development of the Emissive Membrane Ion Thruster.

## References

- 
- <sup>1</sup> Brewer, G. R., *Ion Propulsion*, Gordon and Breach, New York, 1970, pp.102-127.
  - <sup>2</sup> Wilbur, P. J. and Han, J. Z., "Constrained-Sheath Optics for High Thrust-Density Low Specific Impulse Ion Thrusters," *19<sup>th</sup> AIAA/DGLR/JSASS International Electric Propulsion Conference*, May 11-13, 1987, Colorado Springs, CO, Paper AIAA-87-1073.
  - <sup>3</sup> Ibid., Brewer, p. 181.
  - <sup>4</sup> Wilbur, P. J., Wilson, M., Hutchings, K. and Williams, J.D., "The Emissive Membrane Ion Thruster Concept", *29<sup>th</sup> International Electric Propulsion Conference*, Princeton, N. J., Paper IEPC-2005-164.
  - <sup>5</sup> Farnell, C. C., Williams, J. D. and Wilbur, P.J., "Numerical Simulation of Ion Thruster Optics," *28<sup>th</sup> International Electric Propulsion Conference*, Paper 0073-0303, Toulouse, France, March 17-21, 2003
  - <sup>6</sup> Hearn, D. and Baker, M.P., *Computer Graphics, C version*, Prentice Hall, Upper Saddle River, NJ, 1997, pp.327-334.
  - <sup>7</sup> Meadows, G.A. and Free, B. A., "Effect of a Decel Electrode on Primary and Charge-exchange Ion Trajectories," *11<sup>th</sup> AIAA Electric Propulsion Conference*, March 19-21, 1975, New Orleans, LA, Paper AIAA-75-427.